## FABRICATION, TREATMENT, AND TESTING
## OF MATERIALS AND STRUCTURES

# Structure and Properties of Gallium-Oxide Films Produced by High-Frequency Magnetron-Assisted Deposition

**V. M. Kalygina[a],\*, T. Z. Lygdenova[a], V. A. Novikov[a], Yu. S. Petrova[a], A. V. Tsymbalov[a], and T. M. Yaskevich[a]**

*[a] National Research Tomsk State University, Tomsk, 634050 Russia*

*\*e-mail: kalygina@ngs.ru*

**Abstract**—The properties of gallium-oxide films produced by the radio-frequency magnetron-assisted sputtering of a $\beta$-$Ga_2O_3$ target with deposition onto sapphire substrates are studied. The as-deposited gallium-oxide films are polycrystalline and contain crystallites of the $\alpha$ and $\beta$ phases. Exposure to oxygen plasma does not bring about the appearance of new crystallites but makes crystallites several times larger in average dimensions in the substrate plane. After annealing at 900°C, the crystallite size becomes twice as large as that in the unannealed film. The films not subjected to thermal annealing exhibit a high resistance at 20°C. In the range of 50−500°C, the conductivity of the samples ($G$) only slightly depends on temperature ($T$) and, as $T$ is elevated further, exponentially increases with the activation energy 0.7−1.0 eV. After annealing of the films in argon at 900°C (30 min), the conductivity $G$ starts to sharply increase at $T \approx 350$°C. In the dependence of $\ln G$ on $T^{-1}$, a maximum in the range of 470−520°C and a portion of decreasing conductivity at higher temperatures are observed. The unusual temperature dependence of the conductivity after annealing is attributed to a change in the structure and phase composition of polycrystalline gallium-oxide films and, possibly, to some effects at the surface. The structures produced on insulating substrates are solar blind in the visible wavelength region and sensitive to radiation in the ultraviolet region (222 nm).

## 1. INTRODUCTION

Metal-oxide thin films can be single crystal, polycrystalline, or amorphous, depending on the method and conditions of production. Therefore, studying the electrical properties and optical characteristics of such films in combination with their structure presents substantial difficulties.

There exist several approaches to description of the structure, phase composition, and behavior of defects and impurities in oxide films, including $Ga_2O_3$ ones. The mechanism of the conductivity of single-crystal and polycrystalline thin layers of these materials is closely connected with the above-mentioned issue. For example, in studies of gallium oxide, particular interest and discussions are generated by the effect of oxygen, hydrogen, manganese, and some other elements on the electrical, optical, and magnetic properties of the films. The problem is rather hard to solve, since the properties of films depend on the methods of their production and on subsequent technological processes. The results of studies of the same metal oxide materials are often contradictory.

## 2. EXPERIMENTAL

In this paper, we discuss the results of studies of gallium-oxide films produced by high-frequency (HF) magnetron-assisted deposition. 150- to 200-nm-thick films were deposited onto unheated sapphire substrates by the magnetron-assisted sputtering of a $Ga_2O_3$ (99.9999%) target in an $Ar/O_2$ gas mixture, using an AUTO-500 (Edwards) setup. The content of oxygen in the mixture was kept at a level of (56.1 ± 0.5) vol %. The spacing between the target and the substrate was 70 mm. The pressure in the chamber during deposition was $7 \times 10^{-3}$ mbar.

After the deposition of gallium oxide, the substrate with the film was divided into three parts. One part was left without treatment; another part was treated in oxygen plasma at 50°C for 20 min; and the third part was annealed in argon at a temperature of 900°C for 30 min. The structure and phase composition of the gallium-oxide films were determined by X-ray diffraction (XRD) analysis, using a Lab-X XRD 6000 Shimadzu X-ray diffractometer. The surface of the deposited films was analyzed by atomic-force microscopy (AFM), using a Solver HV AFM microscope.
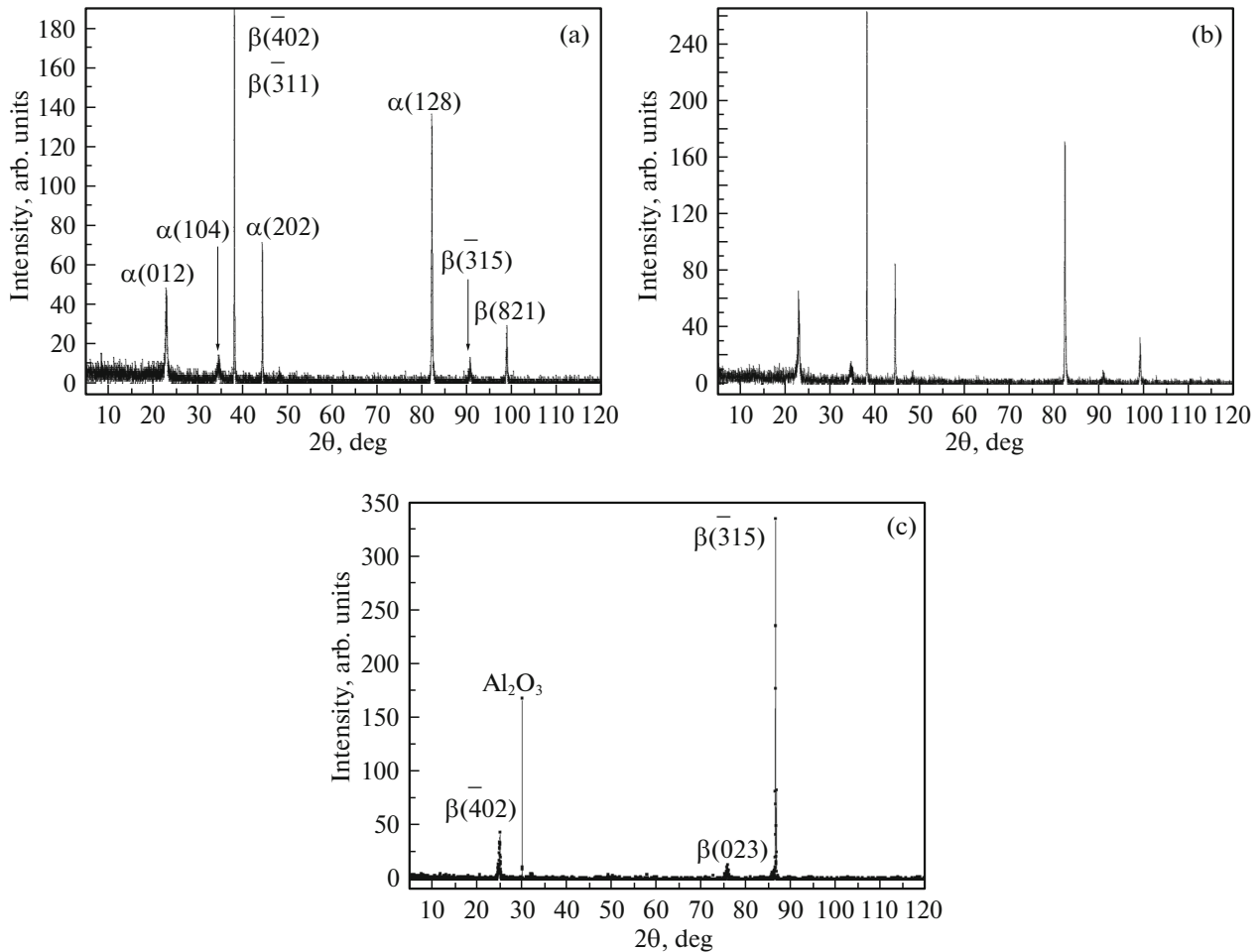
**Fig. 1.** XRD spectra of the gallium-oxide films: (a) unannealed films, (b) unannealed films treated in oxygen plasma, and (c) films annealed in argon at 900°C.

## 3. RESULTS AND DISCUSSION

According to the XRD data, the films produced under the above-described conditions and not subjected to high-temperature annealing are polycrystalline and contain crystallites of the α and β gallium-oxide phases (Fig. 1a).

Oxygen atoms constitute "the material of construction" necessary for the formation of crystallites of various metal-oxide compounds. The content of oxygen in a growing oxide film determines its structure, chemical composition, and electrical and optical properties. For this reason, the produced films were subjected to treatment in oxygen plasma. From comparison of the XRD spectra shown in Figs. 1a and 1b, it follows that treatment in oxygen plasma does not induce the formation of newly oriented crystallites; we observe only an intensification of reflections from crystallites formed upon deposition of the gallium-oxide film by a factor of 1.5. These results differ from the data obtained previously for films deposited by the thermal evaporation of $Ga_2O_3$ powder onto sapphire and semiconductor substrates and for films grown on epitaxial GaAs layers by photostimulated anodization [1, 2].

After annealing in argon at 900°C for 30 min, the crystallites of the α phase disappear from the film, whereas the crystallites of the β phase with different crystallographic planes remain (Fig. 1c).

The inference about the polycrystalline structure of gallium-oxide films not subjected to any treatments is supported by the AFM data (Fig. 2). The average crystallite size is 40 nm (Fig. 2c).

Figure 3 shows the two- and three-dimensional images of the surface of the oxide film not subjected to high-temperature annealing, but treated in oxygen plasma. As a result of treatment in oxygen plasma, the crystallites merge into coarse grains, whose dimensions reach 200 nm (Fig. 3c).

During the lateral growth of crystallites after treatment in oxygen plasma, their average height decreases from 13.5 to 8 nm.
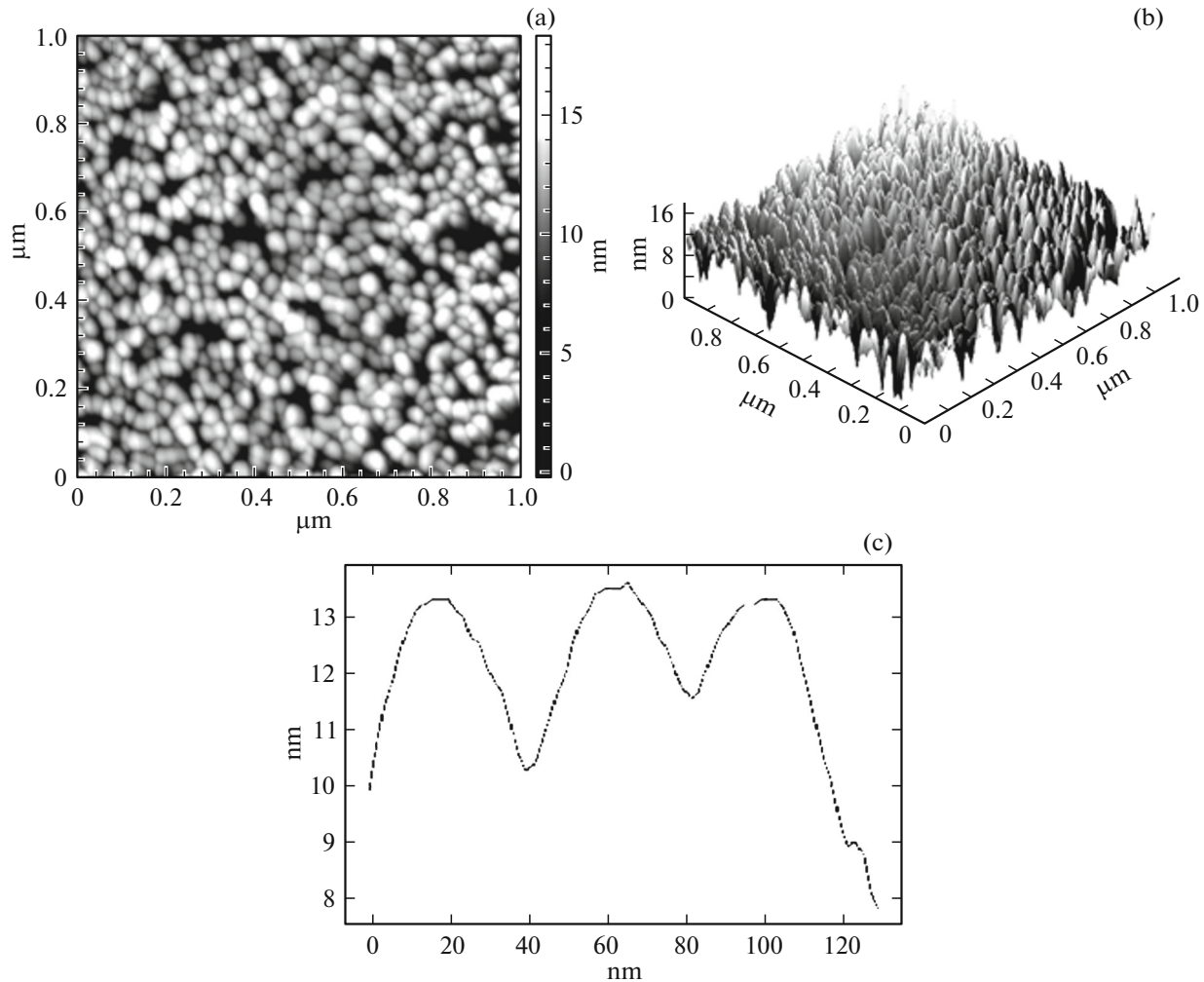
**Fig. 2.** Surface of the oxide film not subjected to high-temperature annealing and treatment in oxygen plasma: (a) the two- and (b) three-dimensional images and (c) the size of the crystallites (relief profile).

After annealing in argon at 900°C, the oxide film contains crystallites, whose average size is 90–100 nm (Fig. 4).

Measurements of the electrical and photoelectric characteristics were conducted for planar samples (Fig. 5). Sample fabrication included several operations: the formation of platinum electrodes and an *n*-shaped heater by means of photolithography; the deposition of a $Ga_2O_3$ film with subsequent annealing in argon at 900°C; the formation of an oxide film by lift-off photolithography; cutting of the substrate into separate $1.4 \times 1.4$ mm$^2$ chips; and soldering of the samples onto a crystal holder. A schematic image of the sample is shown in Fig. 5. The spacing between the electrodes was $2.5 \times 10^{-2}$ cm; the film area between the electrodes was $1.56 \times 10^{-3}$ cm$^2$.

The films formed on sapphire substrates and not subjected to thermal annealing possessed a resistance of ~$(10^9–10)$ Ω. The current–voltage (*I–V*) charac-

teristics of such samples were recorded using an automated complex consisting of a Keithey 2410 meter and a computer. The *I–V* characteristics are described by a linear voltage dependence of the current in the range of electric fields $10^3–10^4$ V cm$^{-1}$.

The temperature dependence of the resistance of the samples in a wide temperature region was studied using special-purpose equipment intended for studies of the electrical and sensor characteristics of devices based on oxide compounds. The system used in the study made it possible to set and maintain the specified temperature and relative humidity in the measurement chamber, into which the four samples were simultaneously placed. The relative humidity in the measurement chamber at all temperatures was kept constant with a special device and corresponded to 32–34% in the experiments of this study.

Figure 6 shows the temperature dependences of the conductivity of the unannealed samples and samples annealed at 900°C. In the range 50–500°C, the con-
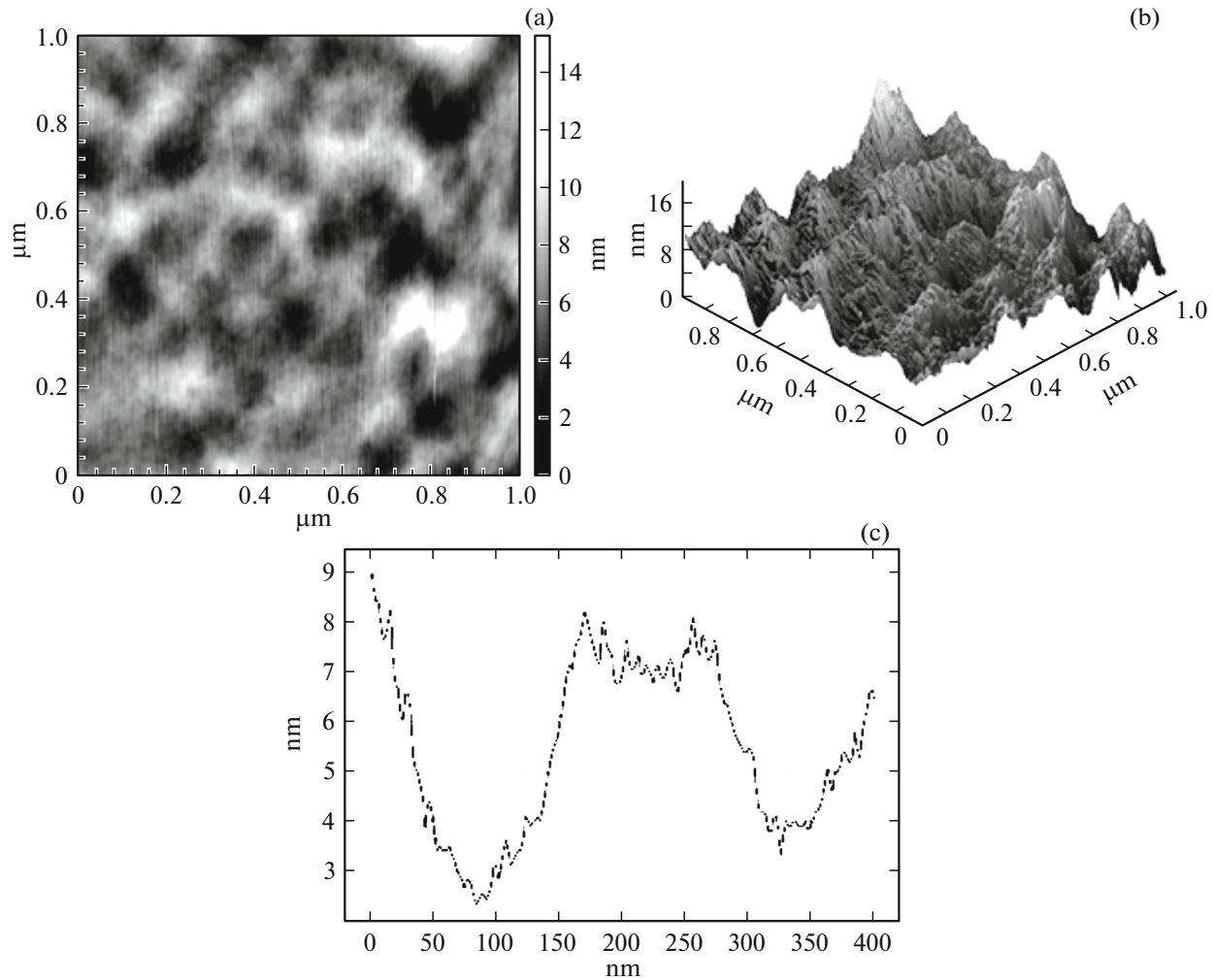
**Fig. 3.** Surface of the oxide film after treatment in oxygen plasma: (a) the two- and (b) three-dimensional images and (c) the size of the crystallites (relief profile).

ductivity $G$ only slightly depends on the temperature $T$ and, as the temperature is elevated further, exponentially increases (Fig. 6a). The activation energy of growth of the conductivity in the high-temperature region is 0.7−1.0 eV.

After annealing the gallium-oxide films in argon at 900°C for 30 min, the region of sharp growth of the conductivity in the temperature dependence $G(T^{-1})$ shifts to lower temperatures, so that sharp growth sets in at $T \approx 350$°C. For most samples, the activation energy of the growth of $G$ with increasing temperature is 0.3–0.5 eV. In the dependence of $G$ on $T^{-1}$, we observe a maximum in the range 470−520°C; at higher temperatures, this maximum gives way to the region of decreasing conductivity.

The unusual shape of the temperature dependence of the conductivity after annealing at 900°C is associated with a change in the structure and phase composition of the polycrystalline gallium-oxide film because of the predominant formation of crystallites of the β phase in the film (Fig. 1c). At the same time, the crystallite size becomes more than twice larger compared to that in the unannealed films (Figs. 2c, 4c).

The low conductivity and its slight temperature dependence in the range from room temperature to 350−520°C can be explained with consideration for the high concentration of defects and for the large contribution of the ionic component to conduction. In this case, the electron transport in the crystal is defined by the hopping mechanism of conduction (see inset in Fig. 6b) [3, 4]. In [5], the hopping mechanism of conduction is attributed to the conduction over disordered grain boundaries.

The increase in the conductivity $G$ with increasing temperature for both the unannealed and annealed samples is most likely due to the activation of electrons trapped at deep energy levels. The nature of such levels is not discussed here.
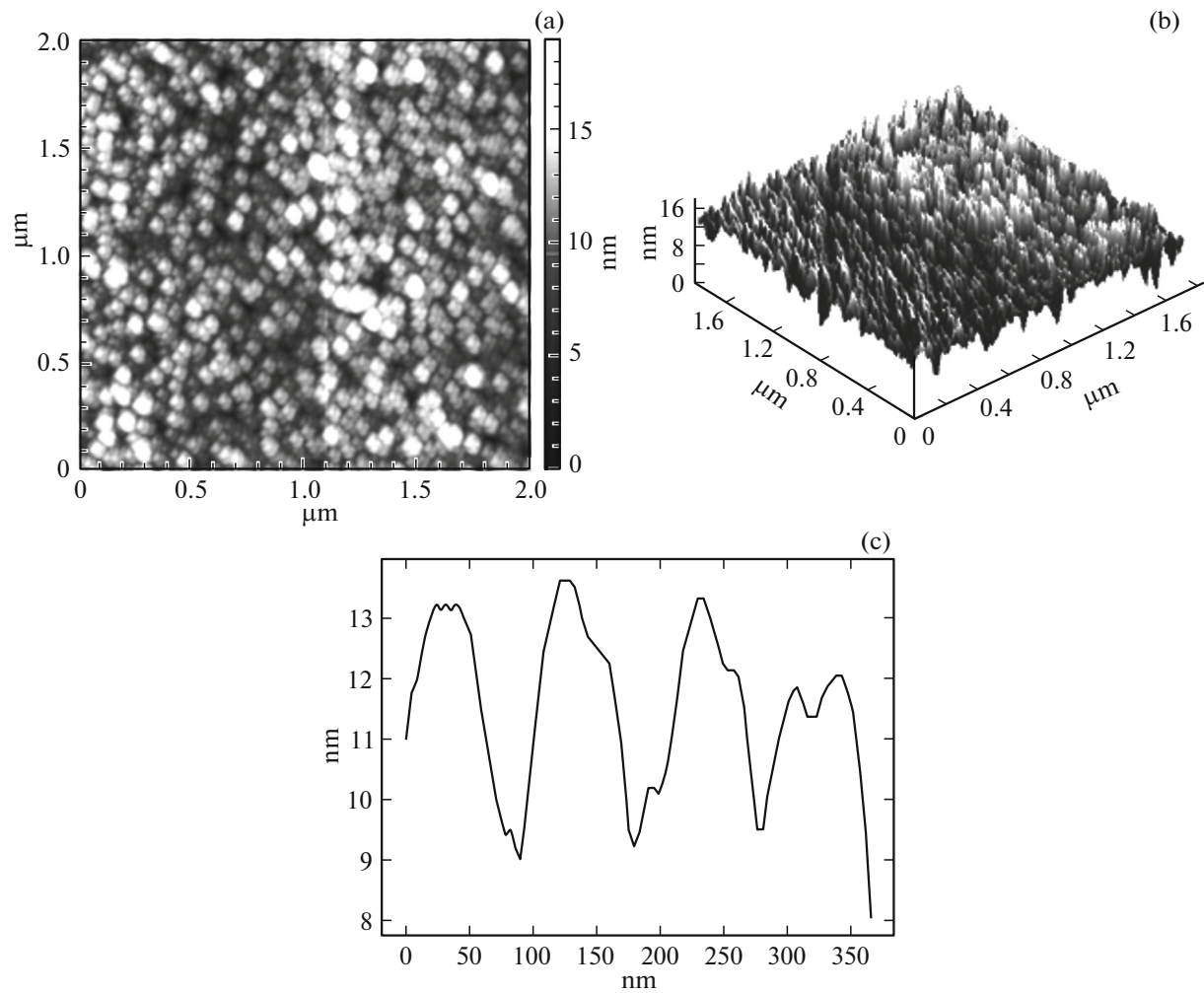
**Fig. 4.** Surface of the oxide film after annealing at 900°C: (a) the two- and (b) three-dimensional images and (c) the size of the crystallites (relief profile).

By analogy with [6], the decrease in the conductivity in the high-temperature region can be attributed to a decrease in the mobility of charge carriers because of



**Fig. 5.** Schematic image of the sample.

their scattering at thermal vibrations of atoms of the crystal lattice. However, at high temperatures, the conductivity decreases in accordance with an exponential law rather than with a power law. At a constant concentration of charge carriers, the conductivity is bound to decrease as $\propto T^{-3/2}$.
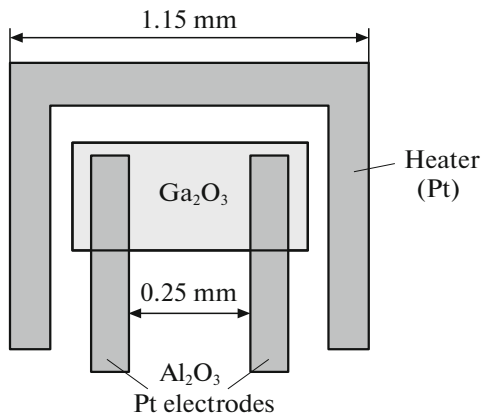
As a rule, it is assumed that, in polycrystalline films, there exist barriers at the boundaries of quasineutral crystallites. The barriers play a certain role in the mechanism of the conductivity of the films, depending on the methods of their production and postproduction technological treatments. Changes in the conditions at grain boundaries can be one of the possible causes of the anomalous temperature dependence of the conductivity of thin oxide films. When the film is in air, oxygen molecules and atoms, water molecules, and hydroxyl groups are adsorbed at the surface of crystallites.

According to [7, 8], there is a negative band bending $e\varphi_s = 0.5$ eV at the surface of $n$-$Ga_2O_3$. Here, $e$ is
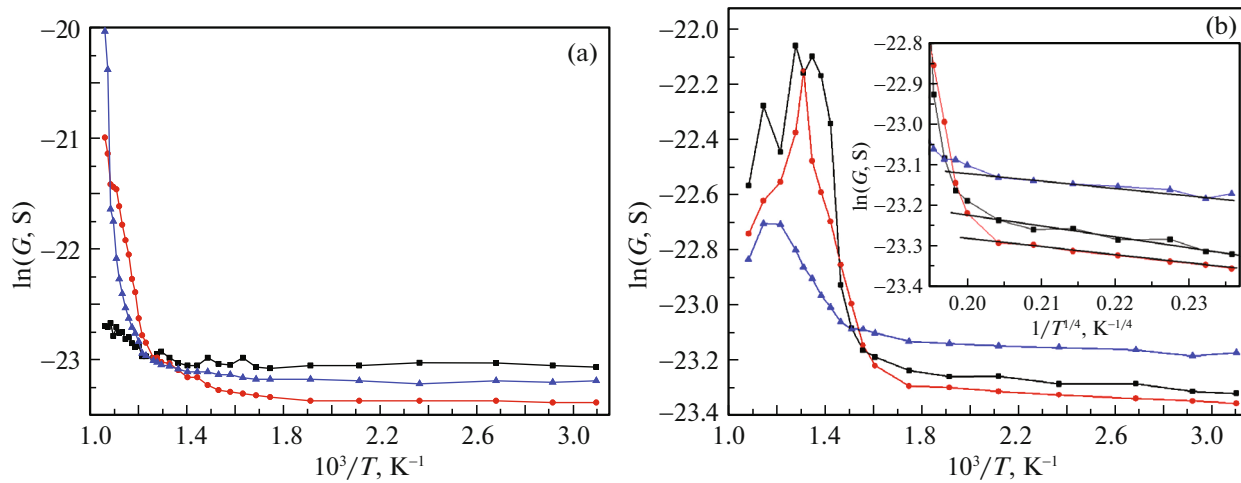
**Fig. 6.** Temperature dependence of the conductivity $G$ of gallium-oxide films on $Al_2O_3$ (a) without and (b) after annealing at 900°C. Inset: temperature dependences of the conductivity plotted as $\ln G$ versus $T^{-1/4}$.

the elementary charge and $\varphi_s$ is the surface potential. The potential $e\varphi_s$ is reckoned from the bottom of the conduction band at the surface, $E_{cs}$, to $E_c$ in the bulk of the film. The bend bending is defined by the concentration of donors $N_d$ and the charge density of ions adsorbed at the surface $eN_i$ [7, 9]:

$$e\varphi_s = \frac{(eN_i)^2}{2\varepsilon\varepsilon_0 N_d} + kT. \qquad (1)$$

Here, $\varepsilon$ is the permittivity of the oxide film, $\varepsilon_0$ is the permittivity of free space, and $k$ is the Boltzmann constant. The negative band bending at the surface of $n$-type gallium oxide results from the trapping of electrons from the conduction band to surface states and from the adsorption of oxygen from the atmosphere.



**Fig. 7.** Current–voltage characteristics of the planar structure without and with exposure to radiation. The wavelengths $\lambda$ are indicated. $D$ denotes the dark current.

As a consequence, each crystallite includes a space-charge layer at the periphery, with the conductivity much lower than that in the bulk. The thickness $d$ of this layer is

$$d = \sqrt{2\varepsilon\varepsilon_0(e\varphi_s - kT)/e^2 N_d}. \qquad (2)$$

At high temperatures, water molecules are desorbed from the film surface, and at $T \geq 400$ K, oxygen adsorbed in the molecular form ($O_2^-$) transforms to the atomic form with the formation of $O^-$ ions. As a result, the negative charge at the surface increases, the width of the space-charge region in the crystallites increases, and the conductivity of the film becomes lower.

The interpretation of the anomalous temperature dependence of the conductivity of gallium oxide films with consideration for surface effects is confirmed by the relation between the thickness of the deposited film and the dimension of crystallite grains after annealing at 900°C. A similar behavior of the temperature dependence of the conductivity was observed in the tin oxide films produced on sapphire substrates by HF magnetron-assisted sputtering [10].

Figure 7 shows the current–voltage characteristics $I-V$ of the planar samples without and with exposure to radiation at the wavelengths $\lambda = 222$ and 400 nm. The dark current is denoted by $D$. From the data shown in Fig. 7, it can be seen that radiation at $\lambda = 400$ nm does not change the $I-V$ characteristic, whereas radiation at $\lambda = 222$ nm induces a noticeable increase in the current that depends on the voltage applied to the sample. The lack of a photoresponse upon exposure to radiation at $\lambda = 400$ nm is most likely due to the fact that the photon energy of this radiation, $h\nu = 3.1$ eV, is smaller than the band gap of gallium oxide $E_g = 4.8-4.9$ eV.
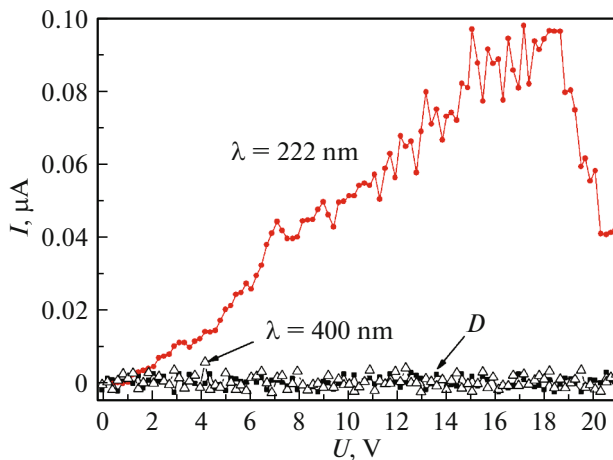
## 4. CONCLUSIONS

The properties of gallium-oxide films deposited onto sapphire substrates by the HF magnetron-assisted sputtering of a $\beta$-Ga$_2$O$_3$ target are studied. From the results, it is possible to draw the following conclusions:

(i) After deposition, the gallium-oxide films are polycrystalline and contain crystallites of the $\alpha$ and $\beta$ phases; treatment in oxygen plasma does not bring about the formation of new crystallites, but increases the average in-plane dimensions of crystallites several times.

(ii) Annealing at 900°C modifies the film surface: the crystallite size becomes twice larger compared to that in the unannealed film.

(iii) The specific features of the temperature dependence of the conductivity of the films after annealing in argon can be the result of surface effects.

(iv) The structures formed on insulating substrates are solar-blind in the visible wavelength region and sensitive to radiation in the ultraviolet region.

## REFERENCES

1. V. M. Kalygina, A. N. Zarubin, Ye. P. Nayden, V. A. Novikov, Yu. S. Petrova, M. S. Skakunov, O. P. Tolbanov, A. V. Tyazhev, and T. M. Yaskevich, Semiconductors **45**, 1097 (2011).
2. V. M. Kalygina, A. N. Zarubin, V. A. Novikov, Yu. S. Petrova, O. P. Tolbanov, A. V. Tyazhev, S. Yu. Tsupiy, and T. M. Yaskevich, Semiconductors **47**, 612 (2013).
3. Z. Zhang, E. Farzana, A. Arehart, and S. A. Ringel, Appl. Phys. Lett. **108**, 052105 (2016).
4. N. P. Zaretskiy, L. I. Menshikov, and A. A. Vasiliev, Sens. Actuators, B **170**, 148 (2012).
5. A. S. Chizhov, M. N. Rumyantseva, and A. M. Gaskov, Inorg. Mater. **49**, 1000 (2013).
6. K. Irmscher, Z. Galazka, M. Pietsch, R. Uecer, and R. Fornari, J. Appl. Phys. **110**, 063720 (2011).
7. A. M. Armstrong, M. H. Crawford, A. Jayawardena, A. Ahyi, and S. Dhar, J. Appl. Phys. **119**, 103102 (2016).
8. T. C. Lovejoy, R. Chen, X. Zheng, E. G. Villora, K. Shimamura, H. Yoshikawa, Y. Yamashita, S. Ueda, K. Kobayashi, S. T. Dunham, F. S. Ohuchi, and M. A. Olmstead, Appl. Phys. Lett. **100**, 181602 (2012).
9. V. I. Gaman, *Physics of Semiconductor Gas Sensors* (NTL, Tomsk, 2012) [in Russian].
10. N. K. Maksimova, E. Yu. Sevast'yanov, N. V. Serge-ichenko, and E. V. Chernikov, *Semiconductor Thin-Film Gas Sensors* (NTL, Tomsk, 2016) [in Russian].

*Translated by E. Smorgonskaya*